



## ORIGINAL ARTICLE

# Comparative research on promising energetic 1,3-diazinane and 1,3-oxazinane structures



Kaidi Yang, Fuqiang Bi, Junlin Zhang, Qi Xue, Jiarong Zhang, Kunkai Wang, Bozhou Wang

State Key Laboratory of Fluorine & Nitrogen Chemicals, Xi'an Modern Chemistry Research Institute, Xi'an 710065, China

Received 15 March 2022; accepted 1 May 2022

Available online 7 May 2022

## KEYWORDS

Chemical diversity;  
Concise synthesis;  
Insensitive energetic materials;  
Melt-cast explosive;  
Eutectic system

**Abstract** The additional carbon centers in 1,3-diazinane and 1,3-oxazinane enable them to covalently bonded geminal-explosophoric groups, leading to unique energetic properties when compared with their homologous energetic structure like RDX. In this paper, a concise synthesis and comparative studies towards 1,3,5-(trinitro1,3-diazinane-5-yl) methyl nitrate and (3,5-dinitro-1,3-oxazinane-5-yl) methyl nitrate (TNOP), two energetic 1,3-diazinane/1,3-oxazinane based promising explosive molecules, are reported. The new germinal nitro/nitroxy explosophoric moieties in the 1,3-diazinane and 1,3-oxazinane frameworks lead to novel structural and energetic properties, which have been investigated through both experimental and computational methods. Densities of the obtained compounds are  $1.83 \text{ g cm}^{-3}$  and  $1.72 \text{ g cm}^{-3}$ , respectively, along with the detonation velocities of  $8714 \text{ m s}^{-1}$  and  $8112 \text{ m s}^{-1}$ . The energetic properties of TNNP are comparable to those of RDX. Meanwhile, the low melting point ( $105 \text{ }^\circ\text{C}$ ) and excellent insensitivity ( $\text{IS} > 60 \text{ J}$ ,  $\text{FS} > 360 \text{ N}$ ) of TNOP make it an ideal material for the preparation of melt-cast explosives.

© 2022 The Authors. Published by Elsevier B.V. on behalf of King Saud University. This is an open access article under the CC BY-NC-ND license (<http://creativecommons.org/licenses/by-nc-nd/4.0/>).

## 1. Introduction

Energetic material is the key component in the developing of advanced explosives and propellants (Zhou et al., 2021; Anbu et al., 2019; Zhang et al., 2016). From structural perspective, most energetic materials are composed of a molecular framework bearing covalently bonded explosophoric groups. The combinations of molecular frameworks and the

explosophoric groups determines the final structural and energetic properties of the energetic materials, and the comparative research on the homologous or similar energetic structures is significant in the understanding of the roles of different molecular frameworks as well as the explosophoric groups (Labarbera and Zikry, 2015; Fu et al., 2022). Early molecular frameworks for energetic materials were based on carbon frameworks, after that, part of the CH or  $\text{CH}_2$  units in carbon frameworks are replaced by N or NH units. Typical examples include cyclotrimethylenetrinitramine (Zhang et al., 2020; Gao et al., 2017) (RDX,  $\rho = 1.80 \text{ g cm}^{-3}$ ,  $D = 8741 \text{ m s}^{-1}$ ) and cyclotetramethylenetetranitramine (Wang et al., 2021) (HMX,  $\rho = 1.89 \text{ g cm}^{-3}$ ,  $D = 9110 \text{ m s}^{-1}$ ), which are still the most important and widely applied energetic materials worldwide (Pang et al., 2020; Chinnam et al., 2020). With a hexahydrotriazinane framework, RDX achieves impressive characteristics of high stability, high enthalpy of formation and high nitrogen content. Similar to hexahydrotriazinane

E-mail addresses: [junlin-111@163.com](mailto:junlin-111@163.com) (J. Zhang), [wzb600@163.com](mailto:wzb600@163.com) (B. Wang)

Peer review under responsibility of King Saud University.



Production and hosting by Elsevier

framework, 1,3-diazinane and 1,3-oxazinane frameworks have also been regarded as promising frameworks for the design and synthesis of advanced energetic materials (Kumar et al., 2012; Yang et al., 2021; Katorov et al., 2009; Yang et al., 2020). Compared with their energetic hexahydrotriazinane derivatives, energetic materials based on 1,3-diazinane and 1,3-oxazinane frameworks exhibit comparable detonation performances but superior structural diversity since different explosophoric groups, like nitro, nitramine and nitroxy, could be implemented together, achieving novel energetic properties. Recently, research towards energetic structures based on the combinations of 1,3-diazinane/1,3-oxazinane frameworks and geminal-explosophoric groups attracted more intensive attentions. For instance, energetic 1,3-diazinane structures like tetranitro1,3-diazinane (Yang et al., 2021) (DNNC,  $\rho = 1.82 \text{ g}\cdot\text{cm}^{-3}$ ,  $D = 8763 \text{ m}\cdot\text{s}^{-1}$ ) showed comprehensive performance equivalent to that of RDX. Meanwhile, energetic 1,3-oxazinane structures, such as 3,5,5-trinitro-1,3-1,3-oxazinane (TNTON,  $\rho = 1.79 \text{ g}\cdot\text{cm}^{-3}$ , m.p. =  $79 \text{ }^\circ\text{C}$ ,  $D = 8322 \text{ m}\cdot\text{s}^{-1}$ ) and 5-azido-3,5-dinitro-1,3-1,3-oxazinane (ADTON,  $\rho = 1.56 \text{ g}\cdot\text{cm}^{-3}$ , m.p. =  $-46 \text{ }^\circ\text{C}$ ,  $D = 7495 \text{ m}\cdot\text{s}^{-1}$ ) showed acceptable performances as potential melt-casting explosive candidate and energetic plasticizer (Xue et al., 2019; Duan et al., 2020); respectively. From a practical standpoint, the synthesis of the frameworks as well as their functionalized derivatives should be concise, reliable and scalable in order to provide a promising foundation for industrial scale-up. However, the applications of all these energetic materials are seriously restricted due to the long synthetic routes and high costs (Katorov et al., 2014; He et al., 2010).

Herein, we reported the first concise synthesis towards 1,3,5-(trinitro1,3-diazinane-5-yl) methyl nitrate (TNNP) and (3,5-dinitro-1,3-oxazinane-5-yl) methyl nitrate (TNOP), in which nitro, nitramino and nitroxy groups are bonded in a single molecular framework. The desired compounds were achieved based on a concise synthesis with low-priced raw materials of nitromethane and formaldehyde. The single crystal structures of TNNP and TNOP were cultured for the first time and analyzed through x-ray crystallography technique; meanwhile, their energetic properties, thermal behaviors and safety performances were investigated through both experimental and computational methods. To further improve the energy of melt cast explosive TNOP, the low eutectic characteristics of TNOP and 3,4-di(3-nitrofuran-4-yl)furoxan (DNTF) were systematically studied. The results show that TNOP and DNTF can form low eutectic, and the energy level is significantly higher than that of TNOP.

## 2. Experimental

**Caution!** Although we have experienced no explosion accident during the synthesis and characterization, adequate protection should be adopted.

### 2.1. Materials and instruments

DNTF used in this study was supplied by Xi'an Modern Chemistry Research Institute.  $^1\text{H}$  NMR and  $^{13}\text{C}$  NMR spectra of TNNP and TNOP were recorded on 500 MHz (Bruker AVANCE 500) nuclear magnetic resonance spectrometers. The samples were dissolved in solvent Acetone- $d_6$ . The melting and decomposition points were determined using a differential scanning calorimeter (TA Instruments Company, Model DSC-Q200) at a flow rate of  $\text{N}_2$  at  $50 \text{ mL min}^{-1}$ . About 0.5 mg of the sample was sealed in aluminium pans for DSC analysis. Infrared spectra were obtained from KBr pellets on a Nicolet NEXUS870 Infrared spectrometer in the range of  $4000 \sim 400 \text{ cm}^{-1}$ . Elemental analysis (C, H and N) were performed on a VARI-El-3 elementary analysis instrument.

The impact and friction sensitivities were determined using the BAM method.

### 2.2. Synthetic procedures

#### 2.2.1. (1,3-Di-tert-butyl-5-nitro1,3-diazinane-5-yl) methanol (DtDNP)

To a stirred solution of nitromethane (0.7 g, 11.5 mmol) in 5 mL water at room temperature, sodium hydroxide solid (0.92 g, 23 mmol) were added to the system for 30 min. Then 37% formaldehyde solution (3.0 g, 37.8 mmol) was added to the mixture and stirred for 3 h. Finally, tertbutyl-amine (1.76 g, 24.1 mmol) was added dropwise over 45 min. The resulting mixture was stirred at room temperature for 20 h. The slight yellow solid DtDNP (1.6 g) was collected by filtration, recrystallized and washed with water with a yield of 51.18%.

$^1\text{H}$  NMR (500 MHz, Acetone  $d_6$ )  $\delta$ :1.01(d, 18H), 2.81(d, 1H), 2.99(dd, 2H), 3.68(dd, 2H), 4.00(d, 1H), 4.50(m, 2H);  $^{13}\text{C}$  NMR (126 MHz, Acetone  $d_6$ )  $\delta$ :25.40, 46.90, 50.32, 52.35, 69.25, 80.90, 88.34; IR (KBr,  $\text{v}/\text{cm}$ ): 3032, 2983, 1553, 1380, 1346, 952, 868, 762; Anal. Calcd. for  $\text{C}_{13}\text{H}_{27}\text{N}_3\text{O}_3$  (%): C 57.14, H 9.89, N 15.38. Found C 57.11, H 9.98, N 15.44.

#### 2.2.2. (1,3,5-Trinitro1,3-diazinane-5-yl)methyl nitrate (TNNP)

5 mL 98% concentrated nitric acid was cooled to  $-5^\circ\text{C}$  in an ice water bath, and 8 mL trifluoroacetic anhydride was added dropwise to the solution. Then a mixture of DtDNP (0.3 g) in 9 mL acetonitrile was slowly added to the acid solution. When the addition was completed, the reaction mixture was allowed to warm to  $25^\circ\text{C}$ , stirring for 8 h, and then poured onto ice. The resulting precipitate was collected by filtration, washed with water, and dried to give a white solid (1,3,5-trinitrohexahydropyrimidin-5-yl)methyl nitrate (0.21 g) with a yield of 64.62%.

$^1\text{H}$  NMR (500 MHz, Acetone  $d_6$ )  $\delta$ :4.47(d,  $J = 16.0 \text{ Hz}$ , 2H), 5.32(s, 2H), 5.38(d,  $J = 14.6 \text{ Hz}$ , 1H), 5.49(d,  $J = 15.0 \text{ Hz}$ , 2H), 7.10–6.89(m, 1H);  $^{13}\text{C}$  NMR (126 MHz, Acetone  $d_6$ )  $\delta$ :48.69, 58.82, 70.88, 83.01; IR (KBr,  $\text{v}/\text{cm}$ ):3083, 3032, 2976, 1567, 1543, 1385, 1344, 1284, 996, 941, 848; Anal. Calcd. for  $\text{C}_5\text{H}_8\text{N}_6\text{O}_9$  (%): C 20.27, H 2.70, N 28.38. Found C 20.57, H 2.93, N 27.98.

#### 2.2.3. (4-Tert-butyl)-5-nitro-1,3-oxazinane-5-yl) methanol (DtNOP)

To a stirred solution of nitromethane (10 g, 66.2 mmol) in 40 mL methanol, t-butylamine(9.6 g, 131.3 mmol) were drop slowly to the solution for stirring 30 min. Then 37% formaldehyde methanol solution (5.3 g, 65.4 mmol) was added in one portion. After reaction for 3 h, the purified product DtNOP (11.1 g, 77.68%) as white crystal was obtained through preparative chromatography.

$^1\text{H}$  NMR (800 MHz,  $\text{CDCl}_3$ )  $\delta$ : 4.35(m, 3H), 4.06(dd, 2H), 3.93(d, 1H), 3.24(dd, 2H), 2.29(s, 1H), 1.10(s, 9H).  $^{13}\text{C}$  NMR (200 MHz,  $\text{CDCl}_3$ )  $\delta$ : 87.28(s), 81.45(s), 68.41(s), 64.70(s), 52.95(s), 49.26(s), 26.56(s). IR (KBr,  $\text{v}/\text{cm}$ ): 3686, 3232, 2976, 2882, 1544, 1485, 1367, 1232, 1153, 1092, 1008, 948, 880, 837, 742, 607. Anal. Calcd For  $\text{C}_9\text{H}_{18}\text{N}_2\text{O}_4$  (%), C, 49.53, H, 8.31, N, 12.84. Found (%), C, 49.38, H, 8.45, N, 12.95.

#### 2.2.4. (3,5-Dinitro-1,3-oxazinan-5-yl)methyl nitrate (TNOP)

The same nitration conditions like TNNP were carried out with the raw materials of DtNOP. After reaction, the acid mixture was poured in the ice and extract with  $\text{CH}_2\text{Cl}_2$ . A slight yellow solid TNOP (0.2 g) were obtained through washing and dry with the yield of 59.82%.

$^1\text{H}$  NMR(500 MHz,  $\text{DMSO}-d_6$ )  $\delta$ :4.38(d,  $J = 12.8$  Hz, 1H), 4.57(d,  $J = 15.7$  Hz, 1H), 4.67(dd,  $J = 12.8$  Hz, 1H), 5.17(dd,  $J = 19.9, 7.8$  Hz, 3H), 5.42(d,  $J = 15.7$  Hz, 1H), 5.85(dd,  $J = 11.5, 0.7$  Hz, 1H);  $^{13}\text{C}$  NMR(126 MHz,  $\text{DMSO}-d_6$ )  $\delta$ :47.96, 68.77, 70.82, 77.33, 83.56; IR(KBr,  $\nu/\text{cm}$ ):3040, 2927, 1668, 1656, 1563, 1535, 1394, 1349, 1279, 1074, 868; Anal. Calcd

For  $\text{C}_5\text{H}_8\text{N}_4\text{O}_8$  (%): C 23.82, H 3.20, N 22.22. Found C 23.85, H 3.26, N 21.91 (see Fig. 1).

### 3. Results and discussion

#### 3.1. Synthesis of TNNP and TNOP

The methods for constructing the framework of 1,3-diazinane and 1,3-oxazinanane from tri(hydroxymethyl) nitromethane or 2-bromo-2-nitro-1,3-propanediol have been reported in our previous research papers (Yang et al., 2021; Xue et al., 2019; Yang et al., 2021). At present, a new two-step synthesis

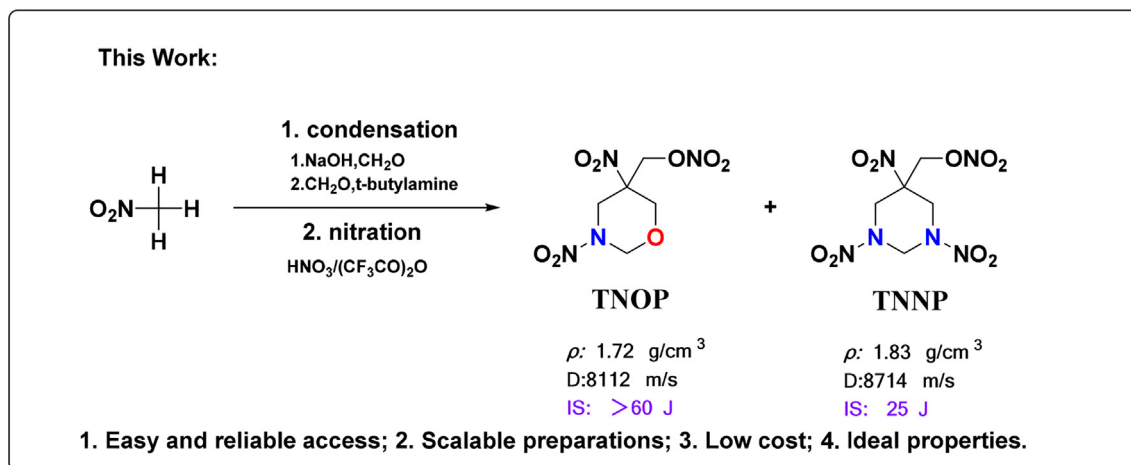
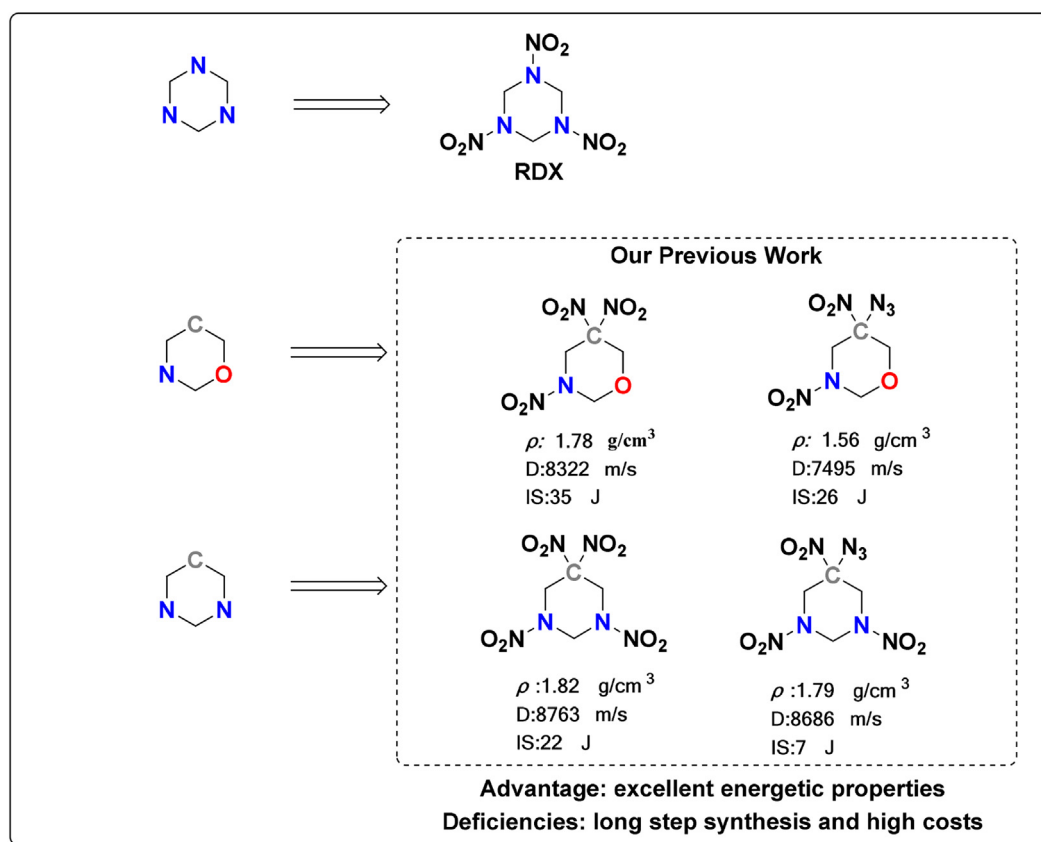


Fig. 1 Representative nitramine energetic compounds.

approach for TNNP and TNOP from simple and readily available raw materials is proposed, and the synthetic pathway is shown in Fig. 2.

By adjusting the amount of *tert*-butylamine, the condensation reaction system can selectively form different skeletons (1,3-diazinane and 1,3-oxazinane). And then the target energetic compounds (TNNP and TNOP) are synthesized in the nitrating system  $(\text{CF}_3\text{CO})_2\text{O}/\text{HNO}_3$ . However, there is a puzzling issue that no target product can be obtained via a number of nitrating reagents, such as  $\text{HNO}_3$ ,  $(\text{CH}_3\text{CO})_2\text{O}/\text{HNO}_3$ ,  $\text{HNO}_3/\text{H}_2\text{SO}_4$ ,  $\text{NH}_4\text{NO}_3/(\text{CH}_3\text{CO})_2\text{O}$ , and  $\text{P}_2\text{O}_5/\text{HNO}_3$ . While nitrating reagents with stronger nitrating capacity could destroy the N-heterocyclic skeleton, systems with weaker nitrating capacity could not replace the *t*-butyl group with energetic nitro group.

### 3.2. Single-crystal X-ray diffraction

Single crystals of the two high-energy and low-sensitivity energetic compounds TNNP and TNOP, which are suitable for X-ray crystal-structure determination, are obtained from mixed organic solvent with ethyl acetate and petroleum ether. The crystal structures of TNNP and TNOP are shown in Fig. 3 (a) and 3(b) with a crystal density of  $1.831 \text{ g}\cdot\text{cm}^{-3}$  and  $1.722 \text{ g}\cdot\text{cm}^{-3}$ . Similar parent skeletons with identical energetic substitution groups may only vary little in crystal structures. TNNP is crystallized in the monoclinic space group  $\text{P}2_1$  with two molecules per unit cell, while TNOP is crystallized in the orthorhombic space group  $\text{Pbca}$  with eight molecules per unit cell (Fig. 3(c) and 3(d)).

According to the crystal structure analysis, the skeletons of 1,3-diazinane and 1,3-oxazinane show chair conformation with a relatively low potential structure. To lower the energy, most substituent groups are located in the equatorial bond. On the contrary, for the germinal nitro and methyl nitrate ester group in C-5, steric effect would be the main factor that places the nitro group in the axial bond. Based on Fig. 3(c) and 3(d), there are abundant hydrogen bonds between molecules and it is the strong interaction force that bonds the molecules

closely. The hydrogen-bond interaction also helps disperse charge and improve stability. Similar to 3(c) and (d), (e) and (f) show regular images, packing layer by layer. For either TNNP or TNOP, the average C—N bond length is about  $1.45 \text{ \AA}$ , shorter than that of a typical C—N single bond ( $1.48 \text{ \AA}$ ). And the average C—C bond length in 1,3-diazinane and 1,3-oxazinane is also  $0.02 \text{ \AA}$  shorter than a typical C—C single bond (Zhang et al., 2020). Shorter single bond length helps stabilize the two parent skeletons. Introduction of the methyl nitrate ester group has greater impact on the 1,3-diazinane skeleton of TNNP. The N—N bond length is quite different ( $1.368 \text{ \AA}$  and  $1.406 \text{ \AA}$ ), mainly due to configuration of the methyl nitrate ester group in C-5. When the group moves closer towards one end, the strong conjugate action would attract the nitro group and cause changes in the bond length.

### 3.3. Hirshfeld and electrostatic potential analysis

Hirshfeld surface analysis and electrostatic potential analysis are two primary means to identify weak intermolecular weak interactions and gain more insights into the relationship between sensitivity and intermolecular interaction (Spackman and Jayatilaka, 2019; Spackman and McKinnon, 2002). Herein, Hirshfeld surfaces of TNNP and TNOP associated with 2D fingerprint spectra are employed to investigate their intermolecular interactions with the results presented in Fig. 4. There are three regions, i.e., red, blue and white, in the Hirshfeld surface, respectively representing longer, closer and the distance of contacts equal to exactly the  $V_{\text{dW}}$  separation with a  $d_{\text{norm}}$  value of zero. The red area appearing on the surface mainly results from intermolecular hydrogen bonds. In comparison of TNNP, TNOP possesses less “hot spots” on its surface, indicating higher stability.

The 2D fingerprint plots can also reveal the relationship between stability and intermolecular interactions. Higher number of O—H and N—H bonds leads to decreasing sensitivity and increasing stability as the interaction force is weaker. O—O interactions usually increase the sensitivity of the ener-

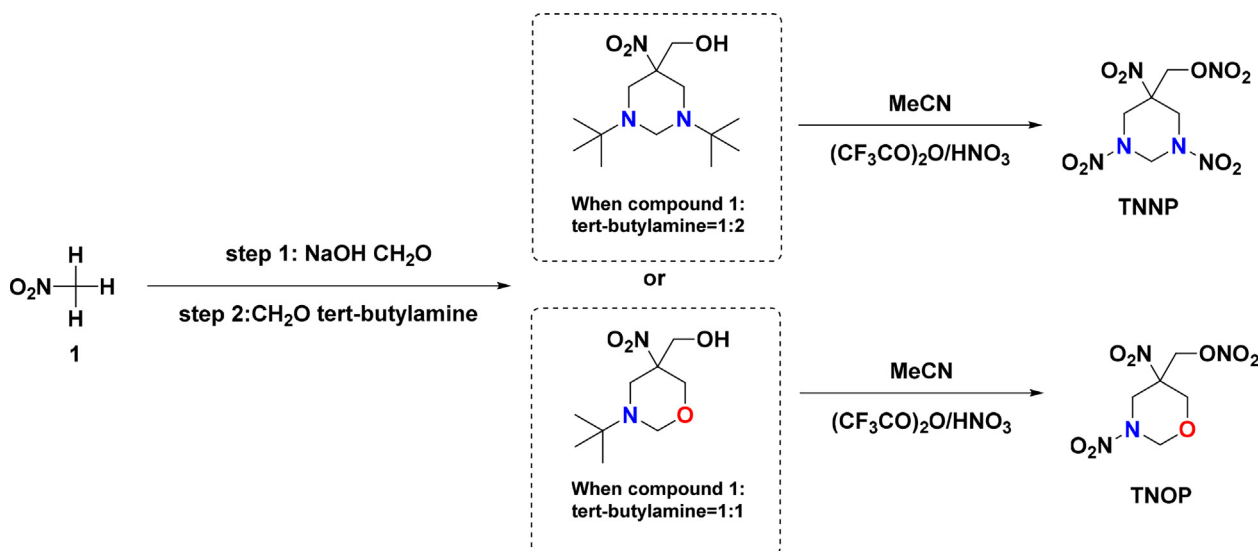
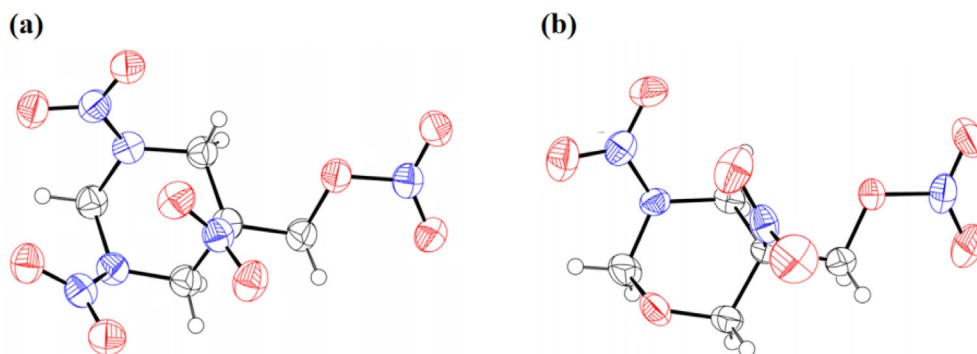


Fig. 2 Synthetic pathway for TNNP and TNOP.



**Fig. 3** (a) Single-crystal X-ray structure of TNNP; (b) Single-crystal X-ray structure of TNOP; (c) 3D crystal structure of TNNP; (d) 3D crystal structure of TNOP; (e) Step-by-step enlarged view of TNNP; (f) Step-by-step enlarged view of TNOP.

getic compound (Zhai et al., 2019; Fischer et al., 2014). As shown in the calculated results, O—H interactions account for 58.8% in TNOP, higher than that in TNNP. In contrast, O—O interactions of TNOP are 22.9%, also lower than 23.3% of TNNP. Compared with other 1,3-diazinane energetic materials we synthesized previously, the Hirshfeld and 2D finger plots indicate that TNNP and TNOP have an acceptable sensitivity performance, which is in good agreement with the crystal analysis and experimental results. Meanwhile, the N—H interactions of TNNP are also much higher than that of TNOP, which could account the high melting point of TNNP as well.

Surface electrostatic potential (ESP) analysis is a universal tool to interpret and predict the reactive behaviors of molecules with high proton-affinity (Murray et al., 1995; Murray et al., 2009; Politzer and Murray, 2015). To clarify the distribution of electrons in similar skeletons and figure out the differences in sensitivity, ESP analysis is conducted for TNNP and TNOP with Multiwfn 3.0.1 based on the Gaussian at B3LYP/6-31 + g(d,p) level with optimized structures (Lu and Chen, 2012). The maximal and minimal values of the potential points are marked as shown in Fig. 5. It is widely accepted that the extent and density of electropositive potential surfaces are positively associated with impact sensitivity. According to the results, negative electrostatic potential is mainly concentrated on C-N and C-O bonds on the 1,3-diazinane and 1,3-oxazinane ring. On the contrary, positive electrostatic potential accumulates around the energetic groups. Due to the more uniform charge distribution and smaller extremum, TNOP shows a better impact sensitivity than TNNP, which could further explain the sensitivity experimental results.

### 3.4. Thermal behaviors

Thermal stability is an important parameter to consider in applications (Kissinger, 1957). The thermal behaviors of TNNP and TNOP are investigated and compared, as shown in Fig. 6. Since TNNP and TNOP have similar nitrogen six-membered heterocyclic framework and the same substituent groups, i.e., C-NO<sub>2</sub>, N-NO<sub>2</sub> and -ONO<sub>2</sub>, they show partial similarity in the thermal behaviors. Tests are conducted by DSC-TG at a heating rate of 10 °C·min<sup>-1</sup> in N<sub>2</sub> atmosphere.

The decomposition processes of TNNP and TNOP are similar, which contain endothermic melting and exothermic decomposition. The melting point of TNNP is 142.7 °C and

its initial one is 134.4 °C, slightly higher than that of TNOP (peak of melting point of 105.3 °C and initial one of 95.5 °C). However, because of the almost the same chemical environment in C-5, which obtain shorter bond of C—N and slightly longer bond of C—O, the thermal decomposition peaks of TNNP and TNOP are almost the same, (201.3 °C and 202.4 °C respectively). Moreover, their initial decomposition points are also approximate, which are 172.2 °C and 174.0 °C. The similar decomposition process is due to the active geminal nitro and nitrate ester group. Lower melting point and higher decomposition temperature make TNOP a promising novel melt-cast explosive. An interesting phenomenon is found that the peak thermal decomposition temperatures of TNNP and TNOP are very similar, probably because they both have nitrate ester groups that are generally considered to be more unstable than nitro groups in energetic materials. When the two compounds are heated, all parts of them are relatively stable except the -ONO<sub>2</sub> that decomposes first, so the decomposition temperatures are similar. From the TG curves, when heated to 400 °C, the residual solid content of TNOP only remains 5.95%, quite lower than that of TNNP. The heat release of TNNP during the decomposition is up to 1435 J·g<sup>-1</sup>, which may be caused by the two high-energy N-NO<sub>2</sub> groups.

To investigate the non-isothermal kinetics during the thermal decomposition of TNNP and TNOP, DSC curves are employed at four different heating rates of 2.5, 5, 10 and 20 K·min<sup>-1</sup>, as shown in Figs. 7 and 8. The peak decomposition temperatures of TNNP at different heating rates are 187.9 °C, 196.1 °C, 202.6 °C and 211.9 °C. And the peak decomposition temperatures of TNOP are 186.8 °C, 194.8 °C, 204.5 °C and 211.4 °C, respectively.

The peak of decomposition temperature of the two compounds increases with the heating rate and the initial decomposition temperature of TNNP is vary from 161.5 °C to 169.3 °C, while for TNOP that is vary from 163.9 °C to 165.4 °C. The kinetic parameters (apparent activation energy (E<sub>a</sub>) and pre-exponential constant (A)) are calculated by applying Kissinger and Ozawa methods using different decomposition points.

Kissinger (Liu, 2021) and Ozawa (Ozawa, 1965) methods are expressed in Eqs. (1) and (2):

$$\ln \frac{\beta_i}{T_{pi}^2} = \ln \frac{AR}{E_k} - \frac{E_k}{RT_{pi}} \quad (1)$$

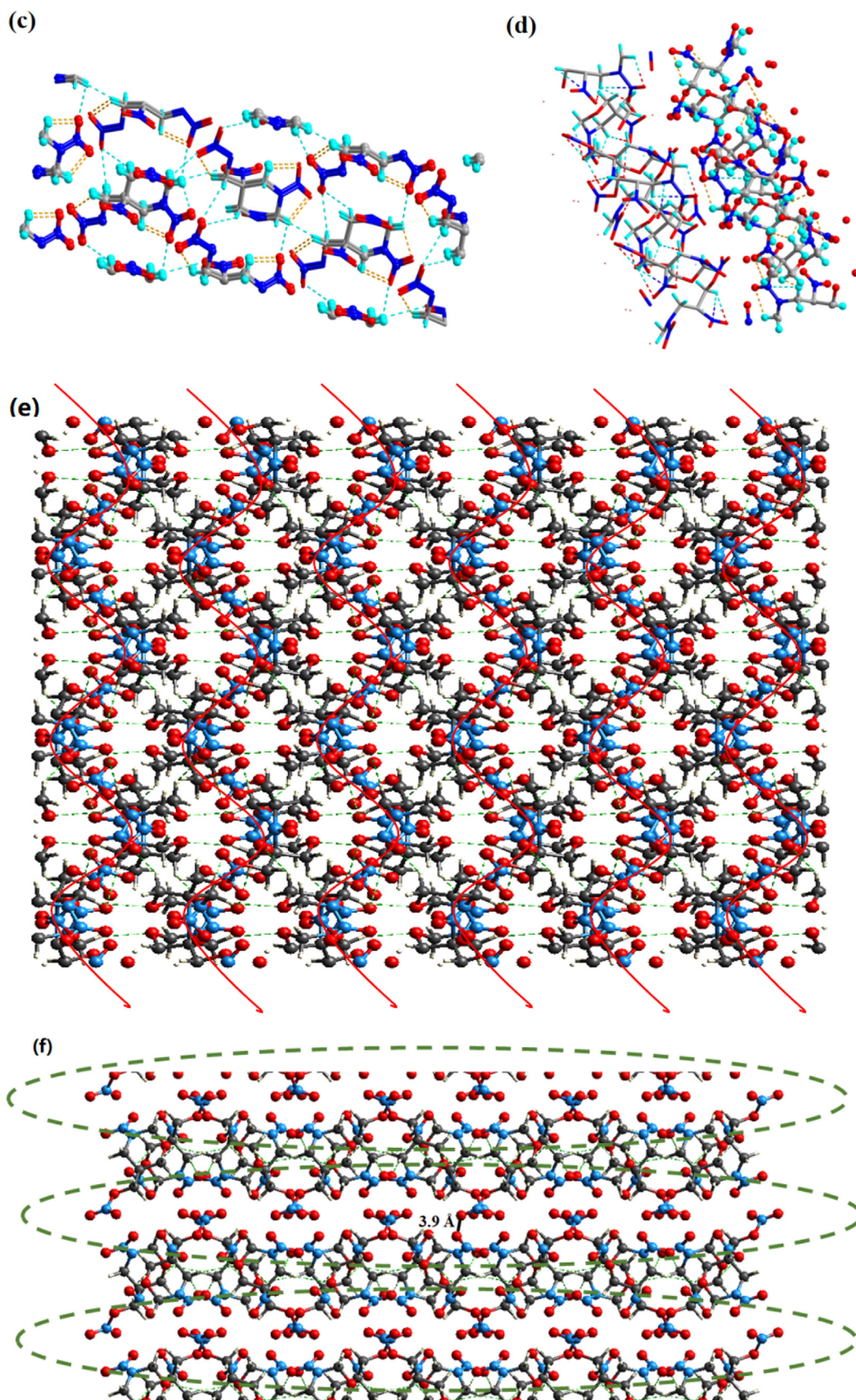
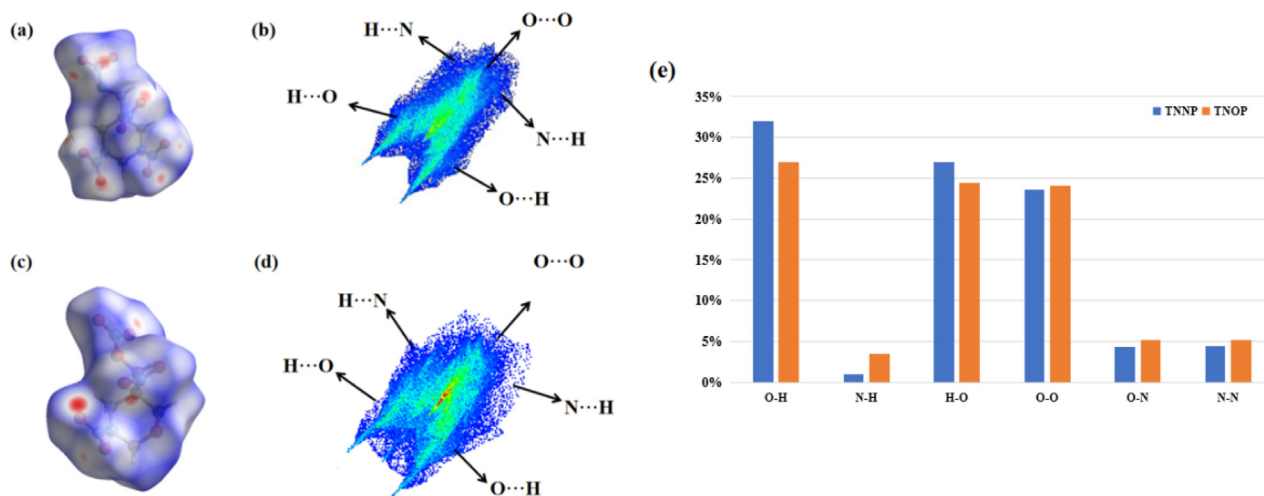
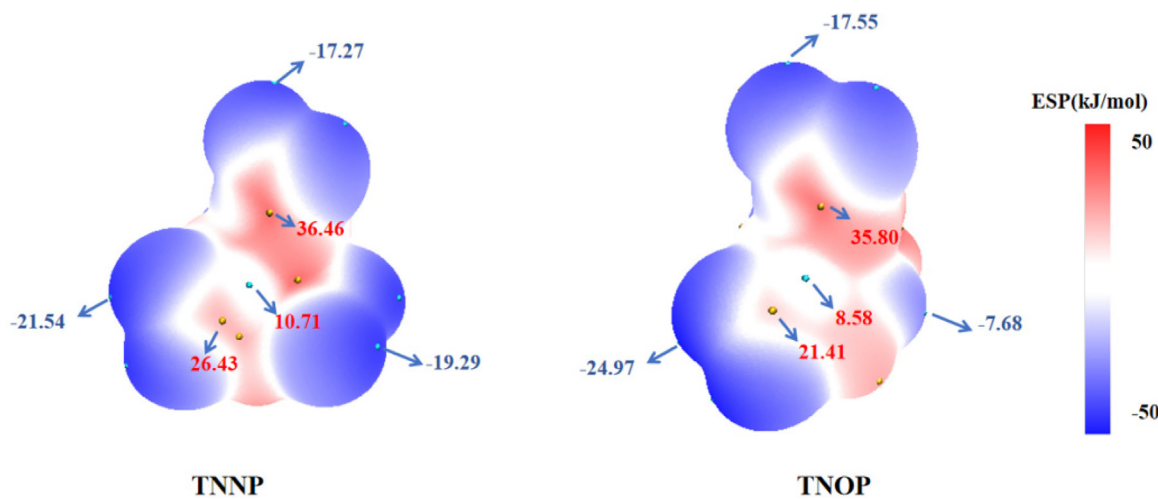


Fig. 3 (continued)



**Fig. 4** (a) Hirshfeld surface of TNNP; (b) 2D fingerprint plot of TNNP; (c) Hirshfeld surface of TNOP; (d) 2D fingerprint plot of TNOP; (e) Comparison of the percentage of close interactions in TNNP and TNOP.



**Fig. 5** Calculated ESPs of energetic compounds: (a) TNNP and (b) TNOP (the value of the isosurface is  $0.001 \text{ e-bohr}^3$ ).

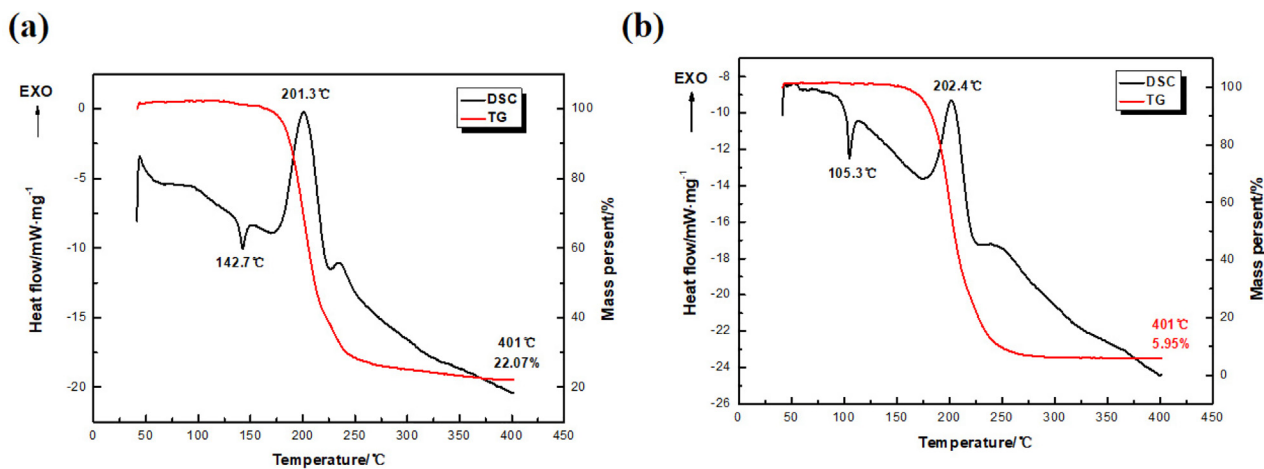


**Fig. 6** DSC and TG curves of (a) TNNP and (b) TNOP.

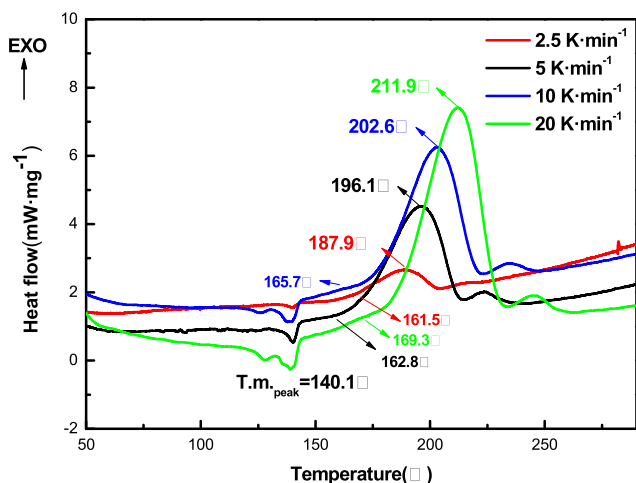


Fig. 7 DSC curves of TNNP at various heating rates.

$$\log \beta_i + \frac{0.4567E_0}{RT_{pi}} = C \quad (2)$$

where  $T_p$  is the peak temperature (K);  $E_x$  is the apparent activation energy ( $\text{kJ}\cdot\text{mol}^{-1}$ );  $\beta$  is the linear heating rate;  $R$  is the gas constant ( $8.314 \text{ J}\cdot\text{K}^{-1} \text{ mol}^{-1}$ );  $A$  is the pre-exponential factor ( $\text{s}^{-1}$ ).

The apparent activation energy  $E_k$  of TNNP obtained from Kissinger's method at atmospheric pressure is  $44.25 \text{ kJ}\cdot\text{mol}^{-1}$ , which is close to  $E_0$  obtained from Ozawa's method ( $42.30 \text{ kJ}\cdot\text{mol}^{-1}$ ). The similar calculation result of  $E_k$  of TNOP is  $47.36 \text{ kJ}\cdot\text{mol}^{-1}$ , only a little higher than that of TNNP. The similar results indicate that both TNNP and TNOP have sound thermal stability.

### 3.5. The bond dissociation energy

Chemical bond dissociation energy (BDE) is usually used to indicate the bond strength (Bach and Schlegel, 2021). The lower the bond's BDE is, the more likely it breaks up during decomposition. TNNP and TNOP are similar in skeleton and possess the same energetic groups. Their sensitivity and stability can be analyzed by calculating the lowest bond disso-

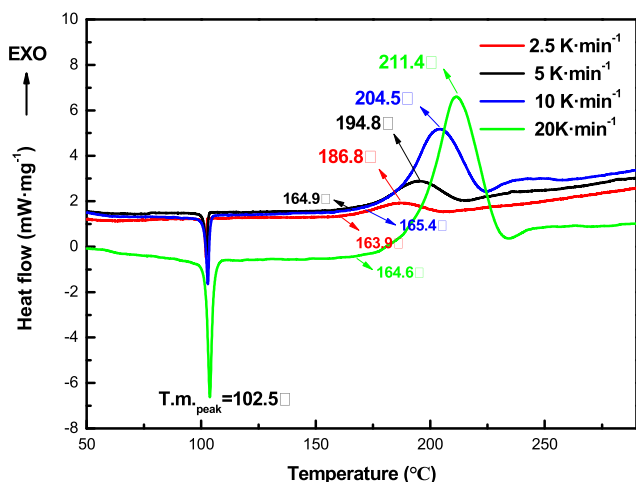


Fig. 8 DSC curves of TNOP at various heating rates.

ciation energy. Two possible bond dissociations have been considered to elucidate the energy threshold with the help of Gaussian 09 at the B3LYP/6-31G(d,p) level and frequency analyses are conducted at the same level of theory for thermal correction (Frisch et al., 2009): (1) the C—NO<sub>2</sub> bond attached to the ring and (2) the O—NO<sub>2</sub> bond among the nitrate ester group. Based on the NBO analysis and practical requirements, the BDE of the two compounds are listed in Table 1.

It is universally accepted that for general energetic materials, to remain thermal stability, BDE should at least exceed  $80 \text{ kJ}\cdot\text{mol}^{-1}$ . Compounds with a BDE higher than  $120 \text{ kJ}\cdot\text{mol}^{-1}$  can be seen as having outstanding thermal behaviors. From Table 1, both TNNP and TNOP exceed  $120 \text{ kJ}\cdot\text{mol}^{-1}$  in BDE, indicating that they can meet the stability requirements. The results also prove that the O—N bond in -ONO<sub>2</sub> is relatively unstable compared to nitro group, which is in great agreement with the fact. Meanwhile, the decomposition temperatures of TNNP and TNOP are almost the same as the two compounds contain the same kinds of energetic groups.

### 3.6. Eutectic mixture

DNTF is a popular explosive with relatively low melting point and exhilarating energetic properties, though its sensitivity is not quite satisfying. The low melting point of TNOP allows it to be mixed with DNTF to acquire higher safety performance while not evidently reducing the energy. By mixing the two, the melting point, oxygen balance and practicability of the explosive mixture are also adjusted. In this paper, 0.5 g of DNTF and TNOP are prepared proportionally as 10:0, 9:1, 8:2 and so on till 0:10. And DSC is used to test the thermal melting and decomposition properties of the mixtures. Results are shown in Fig. 9.

According to Fig. 9(a), there are two melting points, and the first endothermic peak is the melting temperature of the eutectic mixture. The second one is the liquefaction peak of the remaining compounds. Low eutectic points of mixed systems with different proportions are within the range of  $86.8 \text{ }^\circ\text{C}$ – $89.7 \text{ }^\circ\text{C}$ . And the liquefaction peak  $T$  could be corrected by Equation (3) (Frisch et al., 2009; Smith and Pennings, 1976). Based on the DSC results and corrected data, phase diagram of the binary system is built as shown in Fig. 9.

$$T = T'_e - (T_e - T_0) \quad (3)$$

where  $T$  is the corrected liquefaction temperature;  $T'_e$  is the end temperature of liquefaction peak of the mixed system;  $T_e$  is the end temperature of the eutectic peak;  $T_0$  is the starting temperature of the eutectic peak.

Based on Fig. 10, the lowest point of the curve refers to the proper proportion for the lowest eutectic point. When the ratio of TNOP is 64.7% and that of DNTF is 35.3%, the lowest melting temperature is  $95.4 \text{ }^\circ\text{C}$ , much lower than the melting

Table 1 Calculated BDE of TNNP and TNOP.

Compound	—C—O (in nitrate ester)	—O—N (in nitrate ester)
TNNP	$189.7 \text{ kJ}\cdot\text{mol}^{-1}$	$135.4 \text{ kJ}\cdot\text{mol}^{-1}$
TNOP	$290.9 \text{ kJ}\cdot\text{mol}^{-1}$	$144.3 \text{ kJ}\cdot\text{mol}^{-1}$

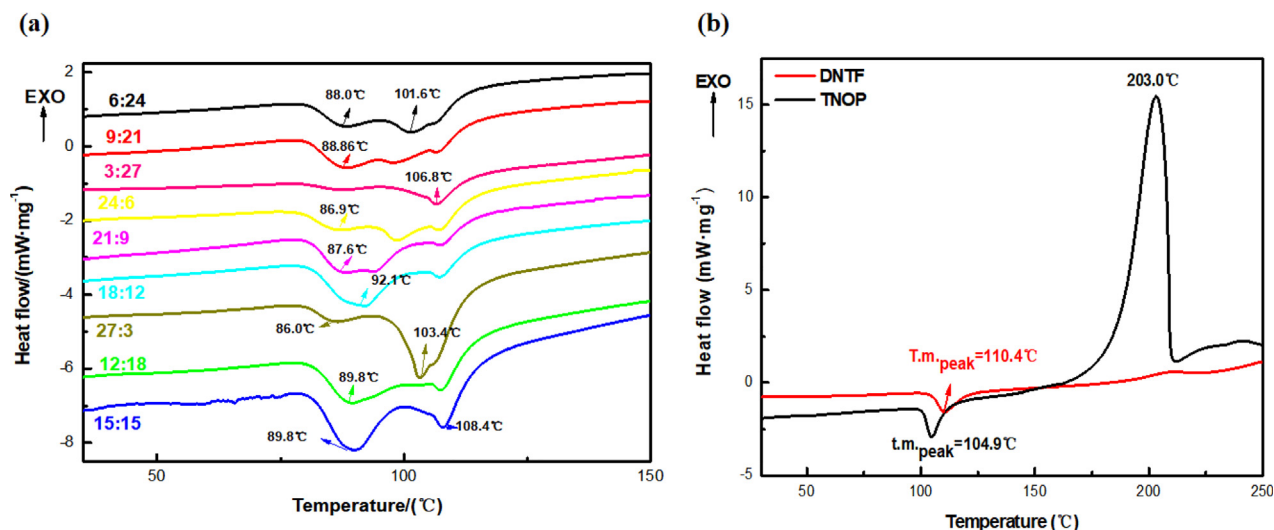


Fig. 9 DSC curves of (a) DNTF/TNOP and (b) TNOP and DNTF mixture systems with different ratios.

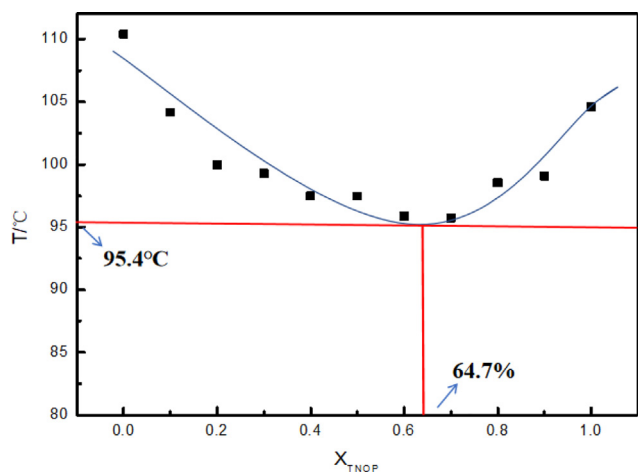


Fig. 10 T-X phase diagram of the TNOP and DNTF binary system.

points of TNOP and DNTF. Meanwhile, the detonation performance of the mixture system is verified using EXPLO5 v6.04 with a density of  $1.79 \text{ g}\cdot\text{cm}^{-3}$ , detonation velocity of  $8230 \text{ m}\cdot\text{s}^{-1}$ , and detonation pressure of  $29.9 \text{ GPa}$ . Though the detonation performance is inferior than that of single-compound DNTF, the system provides a safer melt-cast explosive in applications.

### 3.7. Physicochemical properties, detonation and safety performances

The physicochemical properties, detonation and safety performances matter a lot for the evaluation of energetic materials. For comparison, the properties of TNT and other typical 1,3-diazinane compounds are also analyzed. The gas-phase enthalpies of formation are calculated by Gaussian 09 using the program at B3LYP/6-31 + g (d, p) level of theory, and the enthalpies of sublimation are estimated based on the electrostatic potential parameters. The heat of formation ( $\Delta_f H$ ) of

Table 2 Physicochemical properties, detonation and sensitivity performances of TNNP, TNOP and other materials.

Compound	$\rho^a/\text{g}\cdot\text{cm}^{-3}$	$T_d^b/^\circ\text{C}$	$\Delta_f H^c/\text{kJ}\cdot\text{mol}^{-1}$	$D^d/\text{m}\cdot\text{s}^{-1}$	$P^e/\text{GPa}$	$IS^f/\text{J}$	$FS^g/\text{N}$
TNNP	1.83	201.3	-160.1	8714	34.8	25	260
TNOP	1.72	202.4	-346.6	8112	29.3	> 60	> 360
DNNC <sup>h</sup>	1.82	222.2	308.74	8763	34.9	22	240
DNHM <sup>i</sup>	1.76	197.0	-128.6	8412	31.6	24	240
TNT	1.65	295.0	-67.4	6881	19.5	15	240

<sup>a</sup> Crystal density.

<sup>b</sup> Decomposition temperature (exothermic peak).

<sup>c</sup> Solid phase heat of formation calculated.

<sup>d</sup> Calculated detonation velocity.

<sup>e</sup> Calculated detonation pressure.

<sup>f</sup> Impact sensitivity evaluated using standard BAM fall hammer (Gruhne et al., 2020).

<sup>g</sup> Friction sensitivity evaluated by BAM approach.

<sup>h</sup> 1,3,5,5,-tetranitro1,3-diazinane. <sup>i</sup> 1,3-Dinitrohexahydropyrimidin-5-yl nitrate.

TNNP and TNOP are obtained as  $-160.1 \text{ kJ}\cdot\text{mol}^{-1}$  and  $-346.6 \text{ kJ}\cdot\text{mol}^{-1}$  respectively. Besides crystal density and heat of formation, the general detonation performances are obtained by EXPLO5 v6.04 (Suceska, 2013). Finally, a sensitivity test is also conducted and the results are listed in Table 2.

Compared with TNOP, the molecular arrangement of TNNP is relatively more compact, with a crystal density of  $1.83 \text{ g}\cdot\text{cm}^{-3}$ , which leads directly to higher detonation performance with a detonation velocity of  $8714 \text{ m}\cdot\text{s}^{-1}$  and detonation pressure of 34.8 GPa. Although the energetic level of TNOP is lower than that of TNNP, its sensitivity level is lower and safety performance is much better. The low impact and friction sensitivity make it a promising a novel melt-cast explosive of high safety. Furthermore, the safety performances of all these 1,3-diazinane and 1,3-oxazinane energetic compounds are attributed to the diversity of energetic groups, which regulate certain effects by forming various intramolecular and intermolecular hydrogen bonds.

#### 4. Conclusions

In conclusion, the two energetic materials TNNP and TNOP with superior sensitivity and acceptable energy regulated by C-NO<sub>2</sub>, N-NO<sub>2</sub> and -ONO<sub>2</sub> were synthesized in this paper based on a one-pot synthesis. The low sensitivity and suitable melting point of TNOP makes it a promising melt-cast energetic compound. The crystal structures of TNNP and TNOP were obtained and verified for the first time, and the causes of their low sensitivity and high stability were revealed at the molecular level. Both TNNP and TNOP possess remarkable layered structures due to the regular distribution of multiple chemical bonds. Hirshfeld surfaces of TNNP and TNOP associated with 2D fingerprint spectra were investigated, indicating that the weak interaction force of TNOP was higher than that of TNNP, which highly coincided with the sensitivity data. Composed of the similar skeleton and the same kinds of energetic groups, TNNP and TNOP show similar thermal behaviors with a decomposition temperature of around 202 °C, in agreement with the BDE analysis results. To find out the application prospects of TNOP with satisfying sensitivity and high energy, the eutectic mixtures of TNOP and DNTF at different ratios were prepared and studied by DSC. When the ratio of TNOP was 64.7%, the mixture showed the lowest melting point of 95.4°C. This work provides a solid foundation for the design and synthesis of new low-sensitivity energetic compounds and will drive new explorations in the field.

#### Declaration of Competing Interest

The authors declare that they have no known competing financial interests or personal relationships that could have appeared to influence the work reported in this paper.

#### Acknowledgements

We are grateful to the financial support from National Natural Science Foundation of China (No.21805223) and the China Postdoctoral Science Foundation (No. 2018M633552).

#### Appendix A. Supplementary material

Supplementary data to this article can be found online at <https://doi.org/10.1016/j.arabjc.2022.103947>.

#### References

- Anbu, V., Karunathan, R., Vijayalakshmi, K.A., 2019. Explosives properties of high energetic Trinitrophenyl Nitramide molecules: A DFT and AIM analysis. *Arab. J. Chem.* 12, 621–632.
- Bach, R.D., Schlegel, H.B., 2021. The Bond Dissociation Energy of the N-O Bond. *J. Phys. Chem. A.* 125, 5014–5021.
- Chinnam, A.K., Yu, Q., Imler, G.H., Parrish, D.A., Shreeve, J.M., 2020. Azo- and methylene-bridged mixed azoles for stable and insensitive energetic applications. *Dalton Trans.* 49, 11498–11503.
- Duan, B.H., Liu, N., Lu, X., Mo, H.C., Zhang, Q., 2020. Screening for energetic compounds based on 1,3-dinitro-hexahydropyrimidine skeleton and 5-various explosives: molecular design and computational study. *Sci. Rep.* 10, 18292.
- Fischer, D., Klaptke, T.M., Stierstorfer, J., 2014. Synthesis and characterization of diaminobisfuroxane. *Eur. J. Inorg. Chem.* 34, 5808–5811.
- Frisch, M.J., Trucks, G.W., Schlegel, H.B., 2009. GAUSSIAN 09 Revision A.1. Gaussian, Inc., Wallingford C.
- Fu, Y., Wang, X.J., Zhu, Y., Xu, B., Liu, Z.T., 2022. Thermal characteristics of dihydroxylammonium 5,5'-bistetrazole-1,1'-diolate in contact with nitrocellulose/nitroglycerine under continuous heat flow. *Arab. J. Chem.* 15, 103466.
- Gao, C., Yang, L., Zeng, Y.Y., Wang, X.Q., Zhang, C.C., 2017. Growth and characterization of  $\beta$ -RDX single crystal particles. *J. Phys. Chem. C.* 33, 1761–1766.
- Gruhne, M.S., Lommel, M., Wurzenberger, M., 2020. OZM Ball Drop Impact Tester (BIT2) vs. BAM Standard Method -a Comparative Investigation. *Propell. Explos. Pyrot.* 45, 147–153.
- He, L., Tao, G.H., Parrish, D.A., Shreeve, J.M., 2010. Nitro-cyanamide-based ionic liquids and their potential applications as hypergolic fuels. *Chemistry.* 16, 5736–5743.
- Katorov, D.V., Rudakov, D.F., Zhilin, V.F., 2009. Synthesis of heterocyclic geminal nitro azide. *Russ Chem Bull.* 11, 2311–2317.
- Katorov, D.V., Rudakov, G.F., Katorova, I.N., 2014. Synthesis of 1,2,3-triazoles from heterocyclic  $\alpha$ -nitro azides. *Russ. Chem. Bull.* 45, 2114–2123.
- Kissinger, E.H., 1957. Reaction kinetics in differential thermal analysis. *Anal. Chem.* 29, 1702–1706.
- Kumar, P.M., Kumar, K.S., Mohakhud, P.K., Mukkanti, K., Pal, M., 2012. ChemInform Abstract: Construction of a Six-Membered Fused N-Heterocyclic Ring via a New 3-Component Reaction: Synthesis of (Pyrazolo)pyrimidines/pyridines. *Cheminform.* 43, 431–433.
- Labarbera, D.A., Zikry, M.A., 2015. Dynamic fracture and local failure mechanisms in heterogeneous RDX-estane energetic aggregates. *J. Mater. Sci.* 50, 5549–5561.
- Liu, Z.R., 2021. Review and prospect of thermal analysis technology applied to study thermal properties of energetic materials. *Fire-PhysChem.* 1, 29–138.
- Murray, J.S., Lane, P., Politzer, P., 1995. Relationships between impact sensitivities and molecular surface electrostatic potentials of nitroaromatic and nitroheterocyclic molecules. *Mol. Phys.* 85, 1–8.
- Lu, T., Chen, F., 2012. Multiwfn: A multifunctional wavefunction analyzer. *J. Comput. Chem.* 33 (5), 580–592. <https://doi.org/10.1002/jcc.22885>.
- Murray, J.S., Concha, M.C., Politzer, P., 2009. Links between surface electrostatic potentials of energetic molecules, impact sensitivities and C-NO<sub>2</sub>/N-NO<sub>2</sub> bond dissociation energies. *Mol. Phys.* 107, 89–97.
- Ozawa, T., 1965. A New Method of Analyzing Thermogravimetric Data. *Bull. Chem. Soc. Jpn.* 38, 1881–1886.
- Pang, W., Wang, K., Zhang, W., Deluca, L.T., Li, J.Q., 2020. CL-20-based cocrystal energetic materials simulation, preparation and performance. *Molecules* 25, 4311–4330.
- Politzer, P., Murray, J.S., 2015. Some molecular/crystalline factors that affect the sensitivities of energetic materials: molecular surface

- electrostatic potentials, lattice free space and maximum heat of detonation per unit volume. *J. Mol. Model.* 21, 25–35.
- Smith, P., Pennings, A.J., 1976. Eutectic solidification of the pseudo binary system of polyethylene and 1, 2, 4, 5-tetrachlorobenzene. *J. Mater. Sci.* 11, 1450–1458.
- Spackman, M.A., Jayatilaka, D., 2019. *Cryst. Eng. Comm.* 11, 19.
- Spackman, M.A., McKinnon, J.J., 2002. *Cryst. Eng. Comm.* 4, 378.
- Suceska, M., 2013. EXPLO5, v6.04, Brodarski Institute, Zagreb, Croatia.
- Wang, C., Shang, J., Tian, L., Zhao, H., Li, G., 2021. Direct identification of HMX via guest-induced fluorescence turn-on of molecular cage. *Chin. Chem. Lett.* 12, 4006–4010.
- Xue, Q., Bi, F.Q., Zhai, L.J., Guo, T., Zhang, J.L., Wang, B.Z., 2019. Synthesis, characterization and performance of promising energetic materials based on 1,3-oxazinane. *ChemPlusChem.* 84, 913–918.
- Yang, K.D., Zhai, L.J., Zhang, J.L., Bi, F.Q., Wang, B.Z., 2020. Synthesis and Properties of 1,3-Dinitrohexahydropyrimidin-5-yl Nitrate. *Chin J. Explos Propellants.* 43, 643–648.
- Yang, K.D., Zhang, J.R., Xue, Q., Huo, H., Bi, F.Q., Wang, B.Z., 2021. A Novel Melt-casting Explosive 5-Methyl nitrate-1,5-dinitrooxazine: Synthesis, Crystal Structure and Properties. *Chin J. Energetic Mater.* 29, 272–277.
- Yang, K.D., Bi, F.Q., Xue, Q., Huo, H., Bai, C., Zhang, J.L., Wang, B.Z., 2021. The Synthesis and properties of azamonocyclic energetic materials with geminal explosophores. *Dalton Trans.* 50, 8338–8348.
- Zhai, L.J., Bi, F.Q., Luo, Y.F., Sun, L., Huo, H., Zhang, J.C., Zhang, J.J., Wang, B.Z., Chen, S.P., 2019. Exploring the highly dense energetic materials via regiochemical modulation: a comparative study of two fluorodinitromethyl-functionalized herringbone trifuroxans. *Chem. Eng. J.* 391, 123573.
- Zhang, J.R., Bi, F.Q., Zhai, L.J., Huo, H., Wang, B.Z., 2020. A comparative study of the structures, thermal stabilities and energetic performances of two energetic regioisomers: 3(4)-(4-aminofurazan-3-yl)-4(3)-(4-nitrofurazan-3-yl)furoxan. *RSC Adv.* 10, 31800–31807.
- Zhang, M., Li, C., Gao, H.Q., Fu, W., Li, Y.Y., Tang, L.W., 2016. Promising hydrazinium 3-nitro-1,2,4-triazol-5-one and its analogs. *J. Mater. Sci.* 51, 10849–10862.
- Zhang, J.L., Zhou, J., Bi, F.Q., Wang, B.Z., 2020. Energetic materials based on poly furazan and furoxan structures. *Chin Chem Lett.* 31, 2375–2394.
- Zhou, J., Zhang, J.L., Wang, B.Z., Qiu, L.L., Xu, R.Q., Sheremetev, A.B., 2021. Recent Synthetic Efforts towards High Energy Density Materials: How to Design High-Performance Energetic Structures? *FirePhysChem.* <https://doi.org/10.1016/j.fpc.2021.09.005>.